For office use only	Team Control Number	For office use only
T1 _____	**77845**	F1 _____
T2 _____		F2 _____
T3 _____	Problem Chosen	F3 _____
T4 _____	**A**	F4 _____

2018
MCM/ICM
Summary Sheet

MHPM and MSRSM: Simulation and Modeling of Multi-hop HF Radio Propagation

Summary

Based on the properties of the ionosphere and some laws of physics, we have established a complete mathematical model named MHPM that can well simulate the refraction and reflection in the propagation of multi-hop high-frequency radio waves. MHPM can also simulate the distribution of electron density and refractive index in the ionosphere along altitude. The attenuation of energy in the D layer ionosphere, the "free-space path loss" and the "energy loss while reflecting off the ground or sea surface" determine the energy loss during radio wave propagation, based on which, our model can successfully simulate the loss of energy during the propagation of radio wave.

Using MHPM, we compare the different effects of the calm and turbulent sea surface on the energy dissipation of radio waves, and calculate the maximum propagation distance and the maximum hop number of several cases (different frequencies and different grazing angles). We also analyze the influence of grazing angle, frequency and the wind speed near the sea surface on the refraction effect of rough sea surface. The MHPM can also be applied to ground-reflection situations very well, and we find the energy dissipation of radio waves in ground-reflection case increases rapidly with the increase of elevation standard deviation.

We propose a radio-wave-emission scheme and establish the Moving-Ship-Receiving-Signal Model (MSRSM) in order to make the ship receive signals continuously while sailing on the sea with the same multi-hop path. Applying MSRSM, we simulate the signal receiving process of the moving ship, and get the total duration of 46.20 hours to receive the signal continuously, for a case with the speed of wind near the sea is $20m/s$, the ship speed is $41.67km/h$, and the frequency range is $21MHz \sim 21.45MHz$.

In the sensitivity analysis, we study three factors, which are the electron concentration in the ionosphere, the altitude of the ionosphere and the wind speed near the sea. And we analyze influence of their change on the propagation of multi-hop high-frequency radio waves.

Keywords: multi-hop, MHPM, MSRSM, free-space path loss

Contents

1 Introduction

1.1 Background

HF radio waves can be transmitted in the following three modes: skywave, ground wave, direct wave [1]. The "Multi-hop HF Radio propagation" referred in the MCM's problem A is an application of sky wave.

Skywave which we use in our model is propagated relying the ionosphere which is the high-level (80 to 1000 kilometers above the ground) atmosphere ionized by solar radiation [6]. Because of the multiple reflections off the ionosphere and off the earth, its propagation distance can be very far, generally more than 9600 kilometers [2]. The disadvantage is that it is affected by the climate and the transmission signal is very unstable. The short-wave frequency band is the best of the skywave propagation. **Figure 1** displays the propagation mode.

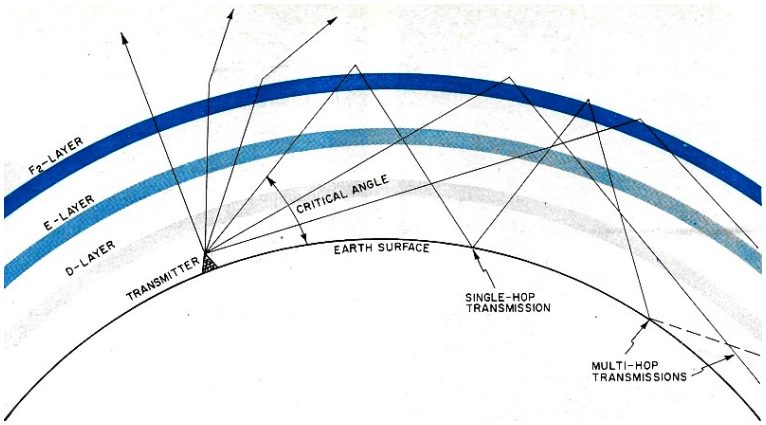

Figure 1: Schematic diagram of Skywave reflection[3]

1.2 Problem Restatement

The problem description has already made a vivid and basic explanation of the transmission patterns of high-frequency skywave bouncing between the ionosphere and the surface of the Earth. After induction and arrangement we distilled the following questions that we need to consider and decide:

- What's factors about ionosphere need to mainly discuss? Solar activity, seasonal change and day or night all have impact on the nature of ionosphere just like density of electrons and the height of the layers.
- What's assuming can not only guarantee the reliability of our model but also simplify it usefully?
- How to quantify the influence of different layers in ionosphere on radio waves? Just like the determination of the reflection, refraction and absorbtion.
- How to quantify the influence of different terrains on radio waves? What's the effects of obstacles on ground? What's the differences between quiet sea and rough

sea? Whether the reflection, angle and attenuation of radio waves will be affected by different surface of earth?

- What's the main factors affecting the signal transmission's distance and the hop-count? And how to calculate the limit distance and the hop-count?
- How can we ensure that our model has a range of coverage? In real navigation, the receiving state changes randomly, and what's method can we take to make radio waves arrive at anywhere in an area whose range can be given accurately?

2 Assumption and Symbols

2.1 Assumption

- The energy loss of radio waves during the "multi-hop" process contains the attenuation of energy in the D layer ionosphere, the "free-space path loss[4]" and "reflection off the ground or sea surface" .
- In solving the problem, if there is no specific description, the wind speed near the sea is 8 m/s (for rough ocean surface), the grazing angle of the electromagnetic wave is 15° and the radio frequency is 20MHz. According to literature [5], the average wind speed on the earth is distributed between $4m/s$ and $12m/s$, so we choose $8m/s$ as a default case.
- The radio wave is simplified as a straight line, like a laser, ignoring the divergence of electromagnetic waves.
- The D layer ionosphere does not affect the propagation path of electromagnetic waves, but will cause the electromagnetic wave energy attenuation, acting as an "attenuation layer" . And the energy loss of electromagnetic waves in the D layer can be calculated by a formula given by Marc C. [1].
- The E layer ionosphere is assumed to cause the refraction of electromagnetic wave only once, does not affect the energy of electromagnetic wave, acting as a "single-refraction layer" .
- The F_1 layer ionosphere and F_2 layer ionosphere [6] are considered as one layer, that is F layer, acting as a "refraction and reflection layer" . The radio wave with appropriate grazing angle and frequency will continuously refract after entering the F layer and then be reflected back to the Earth's surface again.
- We assume that the electron concentration of the E layer is uniform, that is, the refractive index n of E layer is constant. We take the refractive index of the middle height of E layer as its overall refractive index, and assume refraction occurs in the plane at the middle height of the E layer, that is to say, the refraction occurs only once when the electromagnetic wave propagates in the E layer.
- D layer will disappear at night and the density of E layer will decrease by 90% after sunset [1]. In our model, to contain more cases, we only consider the case of daytime, that is D layer is existing, the density of E layer keep constant.

- Only electromagnetic waves with the same frequency can interfere with each other.
- The electromagnetic wave transmitting device and the electromagnetic wave receiving device are reliable and accurate.
- Radio-wave transmitters emit radio waves in a precise way that can emit the radio with the frequency of the target.
- Without a specific description, in our model, the default scenario is daylight during the summer. The wavelength selection of daytime in summer is 20m, 17m or 15m, which means that the frequency selection 15 Mhz, 17.65 MHz or 20 MHz.

2.2 Symbols

Some symbols used in this paper are listed in **Table 1**.

Symbol	Meaning
f	The frequency of the radio waves
n	Refractive index
$N_e(h)$	Electron density of the ionosphere at height h
F_{0E}, F_{0F_2}	The critical frequency of E layer, F_2 layer
y_{mE}, y_{mF_2}	The half thickness of E layer, F_2 layer
h_{mE}, h_{mF_2}	The altitudes of E layer, F_2 layer
N_{mE}, N_{mF_2}	The maximum electron density of E layer, F_2 layer
R_H	The reflection coefficient of horizontal polarization wave
R_V	the reflection coefficient of vertical polarization wave
θ, φ	Grazing angle [7]
v	The wind speed near the sea
c	The speed of light
ρ	The rough correction factor
S_h	The standard deviation of the elevation
λ	The wavelength
K	Boltzmann constant [8], $1.38 \times 10^{-23} m^2 kgs^{-2} K^{-1}$
T_0	The absolute temperature of the environment (in $Kelvin$ [9])
b	The effective noise bandwidth

Table 1: Symbols and their meanings

3 Multi-Hop Propagation Model

3.1 Model Description

In the skywave mode, the refraction and reflection of radio waves in the ionosphere are influenced by the properties of the ionosphere, and the different ionosphere (i.e. D, E, F_1, F_2) are at different altitudes [6] . What's more, their refractive index, thickness, position will change with the alternation of day, night and seasons [1]. MHPM takes

into account the ionospheric effects based on the assumptions presented in the section **Assumption and Symbols**.

According to assumptions, in addition to the attenuation of energy in the D layer, the energy of electromagnetic waves are affected by "free-space path loss[4]" and "reflection off the ground or sea surface" during the "multi-hop" process. And our model contains these factors well. The energy loss caused by the reflection of electromagnetic waves on the surface of the sea or the ground surface is reflected in the **reflection coefficient**, and the reflection coefficients of the calm sea and rough sea surface are discussed in literature [10], what's more, the reflection on the ground from different terrain is discussed in the literature [11]. Our MHPM realizes the simulation and analysis of "single-reflection" process and "multi-hop HF radio propagation" based on the characteristics of electromagnetic waves in the process of propagation and reflection and refraction.

3.2 The Ionosphere

3.2.1 D-Layer Energy Loss

According to literature [1], the energy loss of the radio wave whose frequency is f MHz in D layer is represented as:

$$\alpha = 1.16 \times 10^{-15} \frac{Nv}{f^2} \tag{1}$$

where, α is the energy loss (dB/km), N is the electron density (m^{-3}), v is the collision rate (sec^{-1}), and f is the frequency (MHz). In literature [1], the electron of D layer is very small, so $N = 10^{10}\ m^{-3}$, and the collision rate is $10^6\ sec^{-1}$.

3.2.2 The Refractive Index vs. Altitude and Frequency

Yu Chao et al. analyzed the variation of electron density in ionosphere as well as the refractive index of the ionosphere with altitude and carried out numerical simulation, and the comparison between simulation and real ionospheric data in Sanya City and Wuhan City confirmed the accuracy of their numerical simulation method [12]. So, the refractive index of the ionosphere can be determined by [12]:

$$n = \sqrt{1 - \frac{80.8 N_e}{f^2}} \tag{2}$$

where f is the frequency of the radio wave, and N_e is the electron density, which can be determined by:

$$\begin{cases} N_e(h) = N_{mE}\left[1-(\frac{h-h_{mE}}{y_{mE}})^2\right] & ,h_{mE}-y_{mE}\le h\le h_{mE} \\ N_e(h) = \frac{N_j-N_{mE}}{h_j-h_{mE}}h+\frac{N_{mE}h_j-N_jh_{mE}}{h_j-h_{mE}} & ,h_{mE}\le h\le h_j \\ N_e(h) = N_{mF_2}\left[1-(\frac{h-h_{mF_2}}{y_{mF_2}})^2\right] & ,h_j\le h\le h_{mF_2} \\ N_e(h) = N_{mF_2}exp\left[0.5\times(1-\frac{h-h_{mF_2}}{H}-e^{-\frac{h-h_{mF_2}}{H}})\right] & ,h_{mF_2}\le h\le 1000km \end{cases} \tag{3}$$

where,

$$\begin{aligned} H &= 1.66\left[30+0.075(h_{mF_2}-200)\right],(km) \\ N_j &= 1.24\times10^{10}f_j^2 \\ h_j &= h_{mF_2}-y_{mF_2}\sqrt{1-(\frac{f_j}{f_{0F_2}})^2} \\ f_j &= 1.7f_{0E} \end{aligned} \tag{4}$$

The unit of the electron density is $10^{12}\ m^{-3}$, and the unit of the frequency is MHz. Some ionospheric parameters in the Sanya region are given in the literature [12], and according to B. Zolesi and L. R. Cander, we can get the approximate value of an E-layer maximum electron density [13]. In order to determine the distribution of the refractive index and the electron density along the height, we put these parameters of ionosphere into the **Equation 4, Equation 3, and Equation 2** and can get the graphs of the distribution of the refractive index and the electron density along the height, which is shown in **Figure 2**. All these parameters of ionosphere are shown in **Table 2**.

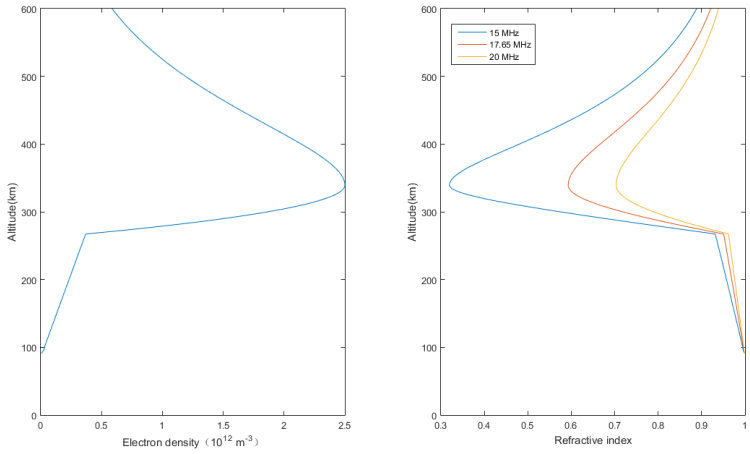

Figure 2: The distribution of refractive index and electron density with altitude

3.2.3 E-Layer Refraction

We assume the refractive index of the area below the middle height of the the E layer is the same as that of the D layer. Because we assume that the D layer only acts as "energy attenuation layer", the refractive index of the D layer is the same as that of the

Parameters	f_{0E}/MHz	h_{mE}/km	y_{mE}/km	f_{0F_2}/MHz
Values	3.21	101	10.7	14.20
Parameters	h_{mF_2}/km	y_{mF_2}/km	N_{mE}/m^{-3}	N_{mF_2}/m^{-3}
Values	339.3	78.0	$10^{10.5}$	2.5×10^{12}

Table 2: Ionospheric parameters used to determine the distribution of refractive index and electron density

air. In order to simplify the calculation, we think that the refractive index of air is 1. The refractive index of the region above the middle height in the E layer is constant, whose value is the refractive index at the middle height. The refraction process in E layer is a simple single refraction, as shown in the **Figure 3**.

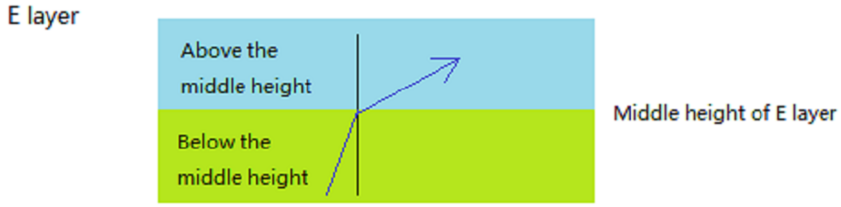

Figure 3: A schematic of the refraction of radio waves in the E layer

3.2.4 F-Layer Refraction and Reflection

The propagation of radio waves in the F layer is complex compared to the E layer because of the reflection of electromagnetic waves in the F layer. We believe that the refractive index of the electromagnetic wave in F layer varies with the altitude, as described in the **Equation 2**. According to the **Figure 2** and **Equation 2**, the refractive index is gradually reduced with the increase of the elevation in F layer, which indicates that the electromagnetic wave will gradually refracted after entering the F layer, and its propagation trajectory will bend. If the electromagnetic wave path is sufficiently curved before reaching the top level of the F layer, it can be reflected back to the ground, otherwise the electromagnetic waves will penetrate the F layer and go out.

Radio waves cannot return to the ground after passing through the F layer. It is because the refractive index is increasing when the altitude is higher than the F layer, as shown in the **Figure 2**, which leads to a decrease in the bending trend of the propagation path of the electromagnetic wave. Thus, it is not possible to bend backwards, that is, to bend back to the ground. This phenomenon is shown in the **Figure 1**.

To show more clearly the propagation of radio waves in the F layer, a schematic diagram **Figure 4** based on the "micro-element method" is shown below:

We take a rather small height as the step h_{step}, dividing the F layer into many parts, each being considered as a micro-element. According to Snell's law [14], we can have:

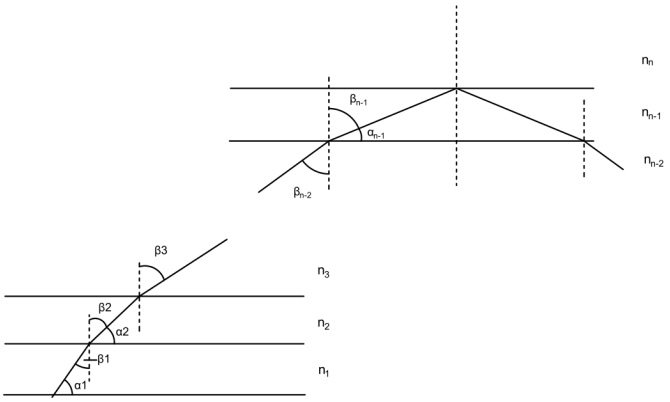

Figure 4: A schematic of the refraction and reflection of radio waves in the F layer

$$\begin{aligned} \frac{n_1}{n_2} &= \frac{sin\beta_2}{sin\beta_1} = \frac{cos\alpha_2}{cos\alpha_1} \\ \frac{n_2}{n_3} &= \frac{sin\beta_3}{sin\beta_2} = \frac{cos\alpha_3}{cos\alpha_2} \\ &\vdots \\ \frac{n_{n-1}}{n_n} &= \frac{sin\beta_n}{sin\beta_{n-1}} = \frac{cos\alpha_n}{cos\alpha_{n-1}} \end{aligned} \tag{5}$$

where, n_i, $i = 1, 2, ...$ can be determined by **Equation 3** and **Equation 2**. So, for each micro-element, i, through **Equation 5** and recursive method, we can get the angle α_i and β_i, then the transverse distance of the radio waves in this micro-element i is:

$$Distance_i = h_{step} tan\beta_i \tag{6}$$

If the radio waves reflect at the m_{th} micro-element, then the overall transverse distance traveled by the radio waves from just entering F layer to the m_{th} micro-elements is:

$$Distance_{total} = \sum_{i=1}^{m} Distance_i \tag{7}$$

where, m can be determined by Snell's law, that is, when $\beta_m = 90°$, it is critical to reflect, and then, the radio waves begin to reflect.

3.2.5 MUF

To achieve the reflection off the ionosphere, the frequency of radio waves must satisfy the limit of critical frequency and MUF. The literature [1] shows a calculation formula of the critical frequency and MUF (maximum usable frequency):

$$MUF = \frac{f_{cr}}{\sqrt{1-(\frac{R_E}{R_E+h})^2}} \\ f_{cr} = \sqrt{\frac{N_e}{1.24\times 10^{10}}} \tag{8}$$

where h is the height of the ionosphere, and the unit of the frequency is MHz. And the typical MUF is $15-40Mhz$ for daytime, $3-14MHz$ for nighttime [1].

3.3 Propagation on The Sea

WANG Ying analyzed the characteristics of the ocean's reflection on the electromagnetic wave, and according to WANG Ying, the reflection coefficient of the surface to the electromagnetic wave can be determined as follows[10]. For smooth ocean surface:

$$R_H = \frac{sin\theta - \sqrt{\widetilde{\varepsilon} - cos^2\theta}}{sin\theta + \sqrt{\widetilde{\varepsilon} - cos^2\theta}} \\ R_V = \frac{\widetilde{\varepsilon} sin\theta - \sqrt{\widetilde{\varepsilon} - cos^2\theta}}{\widetilde{\varepsilon} sin\theta + \sqrt{\widetilde{\varepsilon} - cos^2\theta}} \tag{9}$$

where, $\widetilde{\varepsilon}$ is the complex permittivity of sea surface, which can be determined as: $\widetilde{\varepsilon} = 70 + i300\lambda$, where λ is the radio wave length.

The reflection coefficient of horizontal polarization wave and the reflection coefficient of vertical polarization wave are shown in the **Figure 5** with the change of grazing angle. And the frequencies of the subjects are: $15MHz$, $17.65MHz$ and $20MHz$.

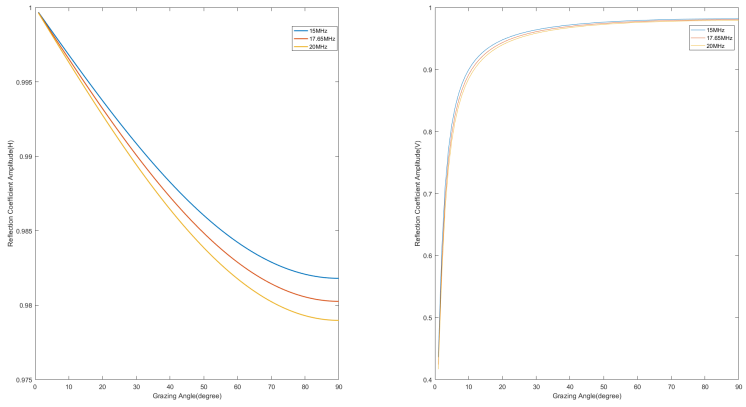

Figure 5: The reflection coefficient varies with the grazing angle, the left one is the horizontal polarization wave, and the right one is the vertical polarization wave

For the reflection of rough sea surface, literature [10] uses the reflection coefficient of smooth sea surface multiplying the rough correction factor to approximate, that is:

$$R' = \rho R \tag{10}$$

where, R' is the reflectance coefficient of rough sea surface, R is the reflectance coefficient of smooth sea surface, and ρ is the rough correction factor, which can be determined by:

$$\begin{aligned} \rho &= \frac{1}{\sqrt{3.2g - 2 + \sqrt{(3.2g)^2 - 7g + 9}}} \\ g &= 0.5(\frac{4\pi h f sin\theta}{c})^2 \\ h &= 0.0051v^2 \end{aligned} \tag{11}$$

The changes of rough correction factor over the grazing angle and the wind speed near the sea surface are shown in **Figure 6**. The **Figure 6** shows that with the increase of grazing angle and the increase of wind speed near the sea surface, the rough correction factor ρ of sea surface decreases gradually. This means that **sea-surface-reflected** sky-wave communication will have better effects when the sea is calmer, and reducing the grazing angle will also enhance the propagation ability of radio waves.

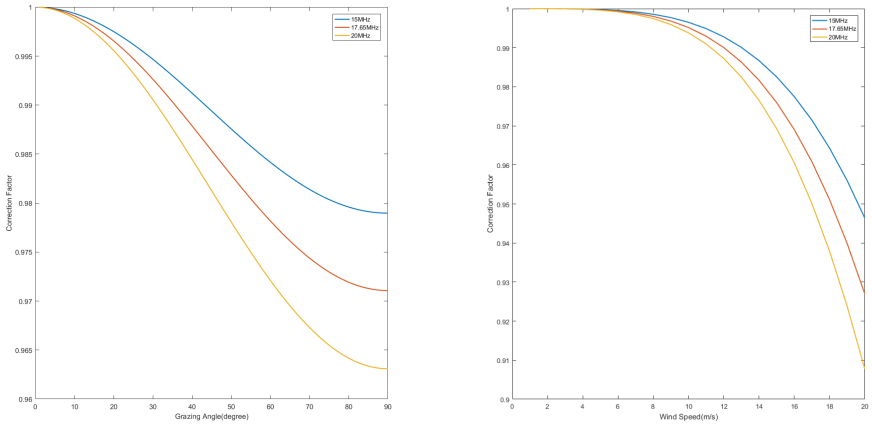

(a) varying with the grazing angle, $v = 8m/s$ (b) varying with the wind speed,$\theta = 15°$

Figure 6: Rough correction factor varies with the grazing angle and the wind speed near the sea surface

3.4 Propagation on The Ground

According to literature [11], the reflection coefficient of electromagnetic wave on flat terrain can still be described by **Equation 9**, which is the equation for calculating the reflectance of sea surface, and the difference is the complex permittivity $\widetilde{\varepsilon}$, which can be determined by $\widetilde{\varepsilon} = \varepsilon_r(f) + i60\lambda\sigma(f)$, where $\varepsilon_r(f)$ is the relative permittivity of the surface at frequency f and $\sigma(f)$ is the conductivity(S/m) of the surface at frequency f.

We take the relative permittivity of the wet concrete as the approximate relative permittivity of the ground surface. According to the literature [15], one can get a approximate range of relative permittivity of wet concrete, 12-18, and we take 15. Literature [16] shows that the electrical resistivity of concrete mainly concentrated in 10-100$\Omega \cdot m$, which means that the conductivity is in 0.01-0.1 S/m, because the conductivity is the reciprocal of electrical resistivity [17], and we take 0.05. So the reflection coefficient of horizontal polarization wave and the reflection coefficient of vertical polarization wave varying over grazing angle can be drawn as **Figure 7**.

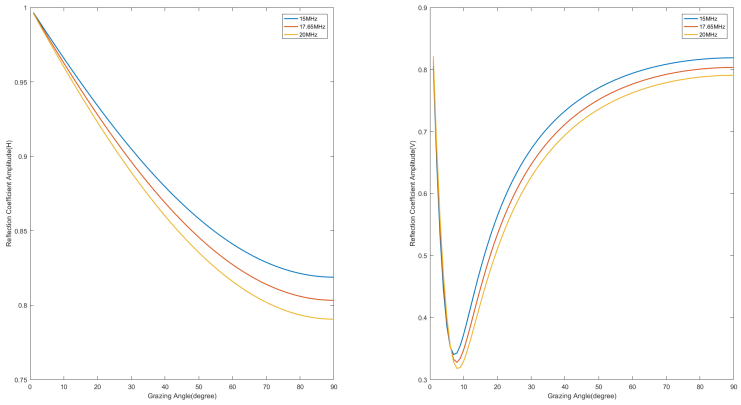

Figure 7: The reflection coefficient of the plane ground surface varies with the grazing angle, the left one is the horizontal polarization wave, and the right one is the vertical polarization wave

For rugged terrain, similar to the situation on the surface of the sea, the refraction coefficient of the plane ground is also multiplied by the topographic reduction factor ρ_s to approximate the real reflection coefficient [11].

$$\begin{aligned} \rho_s = &\quad e^{-0.5g^2} \\ g = &\quad 4\pi(S_h/\lambda)sin\varphi \end{aligned} \tag{12}$$

So we can have the changes of the topographic reduction factor ρ_s over frequency, φ, S_h, which are shown in **Figure 8** and **Figure 9**.

In literature [18], the standard deviation of the elevation, S_h is divided into four categories:

- $0 \leq S_h \leq 10m$, the very flat terrain;
- $10m \leq S_h \leq 30m$, relatively flat meadows;
- $30m \leq S_h \leq 50m$, undulating hills;
- $50m \leq S_h$, mountainous terrain.

As can be seen from **Figure 9(b)**, the rough correction factor decreases rapidly with the increase of elevation standard deviation. When S_h is $15m$, the topographic reduction

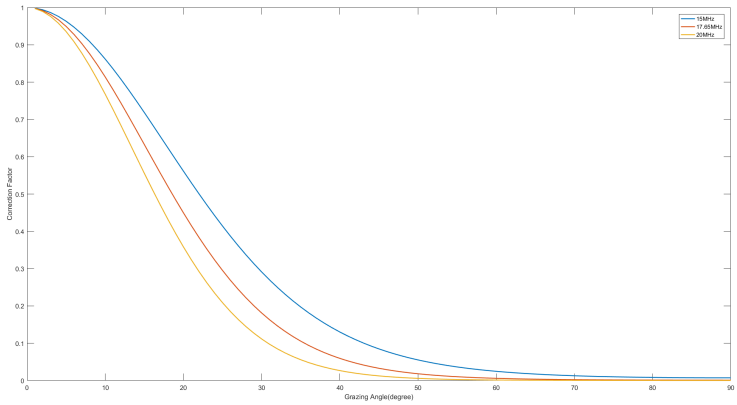

Figure 8: The change of ρ_s over grazing angle

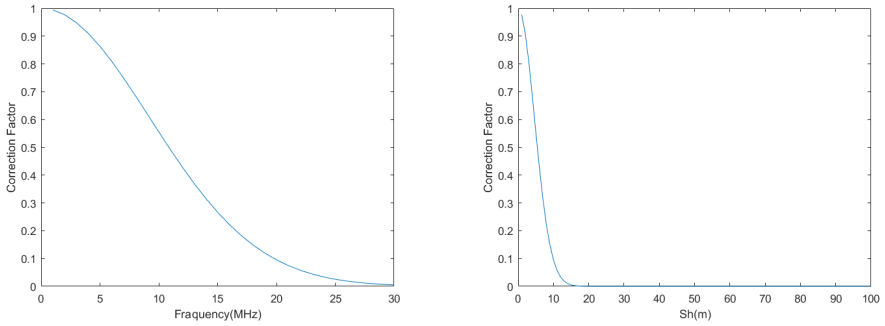

(a) varying with the frequency (b) varying with the S_h

Figure 9: The change of ρ_s over frequency and S_h

factor is almost 0, which means that when the electromagnetic wave is reflected on the ground with large elevation standard deviation, the energy will be greatly lost. **Figure 9(a)** shows that ρ_s decreases as frequency increasing, which means that high-frequency radio waves are more likely to lose energy when reflected on the ground. And **Figure 8** shows that ρ_s can also decrease with the increase of grazing angle, electromagnetic waves with a small incident angle are more likely to lose energy when reflected on the ground. Thus, when using **skywave** to signal transmission on the ground, people should try to choose electromagnetic waves with low frequency, and use smaller grazing angle. At the same time, **ground-reflected** skywave communication is more suitable for flat terrain.

3.5 Free-Space Path Loss

We assume that the energy loss of electromagnetic waves caused by the influence of free-space path loss is always exists as long as the electromagnetic wave is spreading. According to [4], the free-space path loss can be described as:

$$FSPL(dB) = 20log_{10}(d) + 20log_{10}(f) + 32.45 \tag{13}$$

where d id the propagation distance (km) and f is the frequency (MHz).

3.6 Background Noise

We assume that only the background electromagnetic noise which has the same frequency as the target electromagnetic wave can interfere with the radio signal. And according to [19], we get the background noise corresponding to each frequency, whose unit is F_a, which means "dB above KT_0b", that is $10log_{10}\frac{P}{KT_0b}$, where P is the power (Watt) of radio waves, as shown in **Figure 10**.

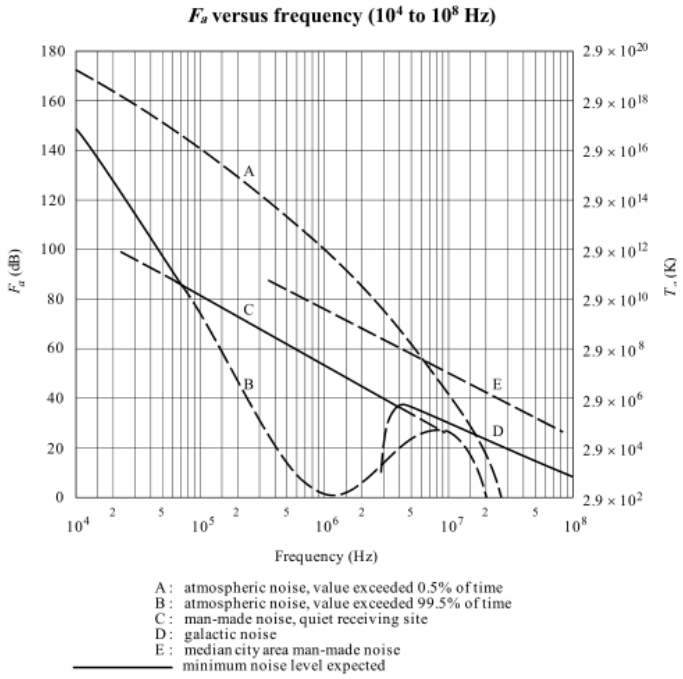

Figure 10: The background noise corresponding to each frequency[19]

4 Result of Part I and Part II

As can be seen from **Figure 7** and **Figure 5**, the reflectance coefficient of horizontal polarization waves are less affected by the change of grazing angle than that of vertical polarization waves, both on the surface of ground and ocean. So, in the model solution, we use the horizontal polarization wave to analyze.

4.1 The Comparison of Strength of Single-Hop Radio Wave Between Calm and Turbulent Ocean Surface

We simulate a single-hop radio wave, and get the strength (in dBw [20]) of the wave after the first reflection from the turbulent ocean surface and the calm ocean surface. Several cases of radio waves with different frequencies, wind speeds and grazing angles are shown in **Table 3**. In addition, we draw the changes of the power ratio between the waves on turbulent and calm ocean surfaces with grazing angle and the wind speed near the sea surface, as shown in **Figure 11**.

Cases	$Power_c\ (dBw)$	$Power_t(dBw)$	Diff.(dBw)	Power ratio
$20MHz, 15°, 8m/s$	47.666	47.644	0.022	1.005
$17.65MHz, 15°, 8m/s$	45.634	45.617	0.017	1.004
$20MHz, 25°, 8m/s$	56.347	56.288	0.059	1.013
$20MHz, 15°, 16m/s$	47.666	47.316	0.350	1.084

Table 3: A show of some cases of the comparison of the wave strength between calm and turbulent surfaces, where $Power_c$ means the power(in dBw) of the calm-surface case, and $Power_t$ means the power(in dBw) of the turbulent-surface case, Diff. means the difference between $Power_c$ and $Power_t$

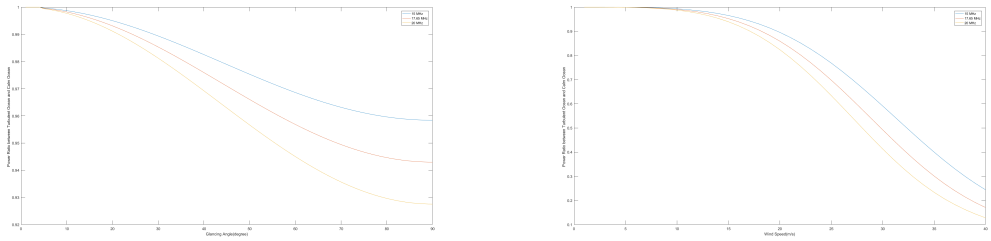

(a) varying with the grazing angle (b) varying with the wind speed

Figure 11: The changes of the power ratio between the waves on turbulent and calm ocean surfaces with grazing angle and the wind speed near the sea surface

4.2 The Multi-Hop Radio Propagation Process on Ocean Surface

According to the model, we simulate the multi-hop radio propagation process on the sea surface, and draw the pictures of the propagation process with varying grazing angle and varying frequency, as shown in **Figure 12**.

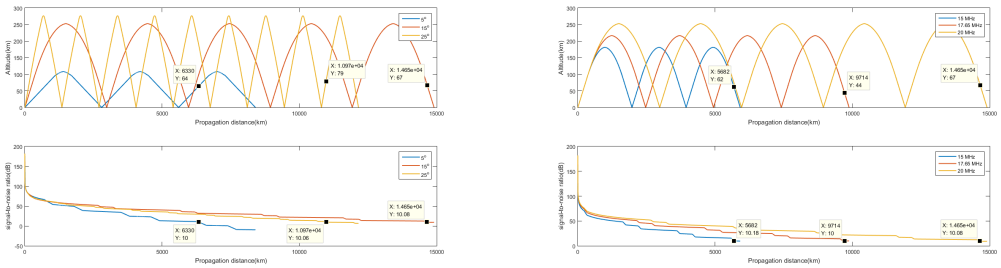

(a) varying with the grazing angle (b) varying with the frequency

Figure 12: A show of the propagation process with varying grazing angle and varying frequency, in 12(a) the frequency is $20MHz$, and in 12(b) , the grazing angle is $15°$

We call the electromagnetic wave up and down as a hop. As shown in the **Figure 12**, we get the number of hops and the maximum propagation distance of each case, as shown in **Table 4**.

$20MHz$	No. of hop	D(km)	$15°$	No. of hop	D(km)
$5°$	2	6300	$15MHz$	2	5682
$15°$	4	14650	$17.65MHz$	3	9714
$25°$	8	10970	$20MHz$	4	14650

Table 4: A shown of the number of hops and the maximum propagation distance of each case shown in **Figure 12**, D means the maximum propagation distance

4.3 The Comparison of Strength of Single-Hop Radio Wave Between Rugged and Smooth Ground Terrains

Similar to the **sea-surface-reflected** case, we do the comparison of the strength of the waves that are reflected from ground surface between rugged and smooth ground terrains. Because the ground surface has a great effect on the dissipation of electromagnetic energy, which can be seen from **Figure 9**, we only analyze the single-hop case. **Table 5** shows the **radio-wave power ratio of rugged surface to smooth surface** in several cases. And **Figure 13** indicates the change of the power ratio of rugged surface to smooth surface with the standard deviation of the elevation, S_h.

Cases	$Power_s$ (dBw)	$Power_r(dBw)$	Diff.(dBw)	Power ratio
$20MHz, 15°, S_h = 5$	47.186	42.081	5.105	0.309
$20MHz, 15°, S_h = 10$	47.186	26.768	20.418	0.009
$20MHz, 15°, S_h = 15$	47.186	1.245	45.941	2.547E-5
$20MHz, 15°, S_h = 20$	47.186	-34.486	81.672	6.804E-9

Table 5: A show of some cases of the comparison of the wave strength between rugged and smooth ground terrains, where $Power_s$ means the power(in dBw) of the smooth-surface case, and $Power_r$ means the power(in dBw) of the rugged-surface case, Diff. means the difference between $Power_s$ and $Power_r$, Power ratio is ratio of rugged-surface power to smooth-surface power

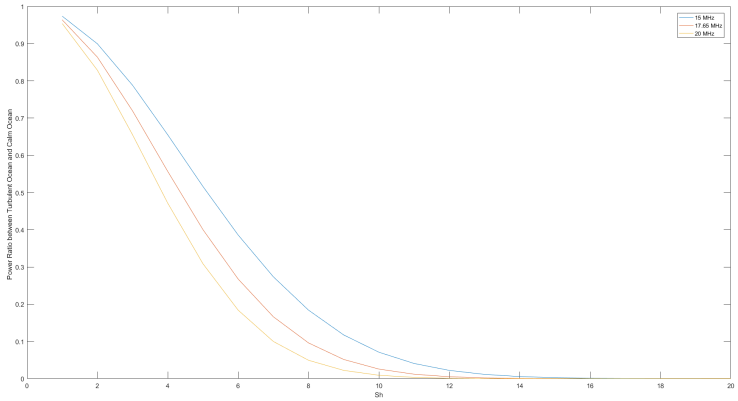

Figure 13: A show of the change of the ratio of rugged-surface power to smooth-surface power with S_h

5 Moving-Ship-Receiving-Signal Model

In order to ensure that the ship can continue to receive signals at sea, we assume that radio waves are not a single frequency at launch, but have a certain bandwidth. For example, the frequency of the emitted waves consists of all frequencies between $21MHz$ and $21.45MHz$.

Because the frequency of electromagnetic waves in a given frequency range is continuous, and electromagnetic waves with different frequencies will have different propagation path, the intersection of electromagnetic waves and the sea is no longer a point, but becomes a range. We take the length of this range as L, and take the speed of the ship as v_{ship}, then, the ship can remain in communication using the same multi-hop path for $time = \frac{L}{v_{ship}}$.

6 Result of Part III

Based on the Moving-Ship-Receiving-Signal Model (MSRSM), we analyze the length of time the ship can remain receiving signal with the same path, and for the speed of ship, the wind speed near the sea surface, the frequency range, we take $41.67km/h$, $20m/s$, $21MHz - 21.45MHz$, respectively. The grazing angle is $15°$. A show of the multi-hop propagation process of the continue-frequency radio waves is given in **Figure 14**.

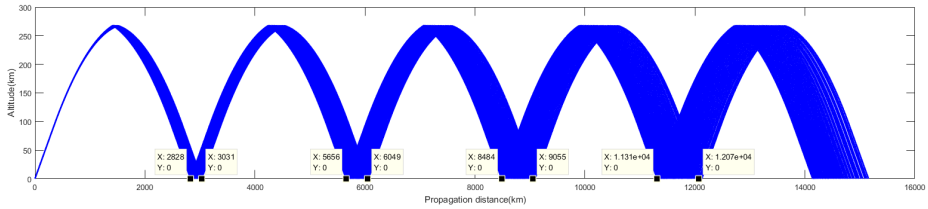

Figure 14: A show of the multi-hop propagation of the continue-frequency radio waves, with speed of wind near the sea is $20m/s$, and the ship speed is $41.67km/h$, and the frequency range is $21MHz - 21.45MHz$

Then we analyze the length of each intersection zone (km), and get the length of time (hour) the ship can remain receiving signal in each intersection area, as shown in **Table 6**.

Intersection zone	Left(km)	Right(km)	Length(km)	Time(hour)
1	2828	3031	203	4.87
2	5656	6049	393	9.43
3	8484	9055	571	13.70
4	11312	12070	758	18.19
total			1925	46.20

Table 6: A show of the length of time a ship can remain getting signal in each intersection area

7 Sensitivity Analysis

Solar activity, seasonal change, day and night will affect the nature of the ionosphere around the earth, such as the altitude of the ionosphere, the density of electrons, and so on [6]. We analyze the effects of these factors on the propagation of the multi-hop HP radio waves.

7.1 Electron Density of The E Layer and F Layer

According to **Equation 3**, we change the electron density distribution of E and F layers by changing the maximum electron density of E and F layers. **Figure 15** indicates the effect of the change of the maximum electron density of E Layer and that of F layer. As can be seen from it, the increase in E-layer electron density makes the radio waves spread farther, because the increase in E-layer electron density makes the refractive index of the E layer decrease, which means that the bending trend of electromagnetic waves in the E layer will become larger, and the radio waves will spread farther in the horizontal direction. In addition, the loss of energy in the process of transmission has hardly changed. However, the change of the maximum electron density of the F layer hardly affects the propagation process of radio waves, because the change of the maximum electron density of the F layer has no effect on the electron concentration in the lower layer of F layer, only affects the electron concentration in the upper part of F layer, that can be got by analyzing the **Equation 3**. And in the examples analyzed in this section, no electromagnetic waves reach the upper part of F layer.

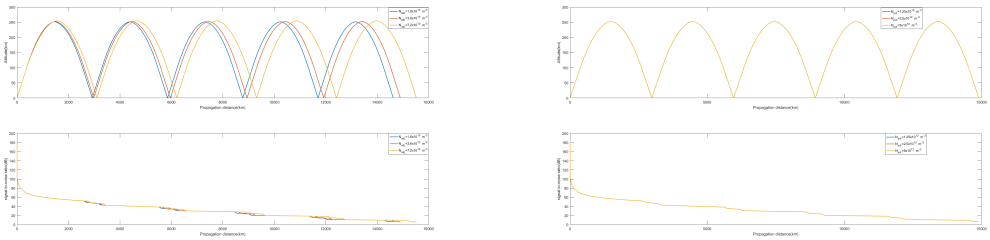

(a) change the electron density of the E layer (b) change the electron density of the F layer

Figure 15: A show of the radio-wave propagation process with the change of electron density distribution of the E and F layers

7.2 The Height of The F Layer

We analyze the propagation of the multi-hop HP radio waves with the height of the F layer is 289.8m, or 339.3m, or 418.6m. As shown in **Figure 16**, as the altitude of the F-layer ionosphere increases, radio waves can travel higher and the maximum propagation distance is increased. However, the maximum number of hops does not change, and the propagation paths looks similar in geometry.

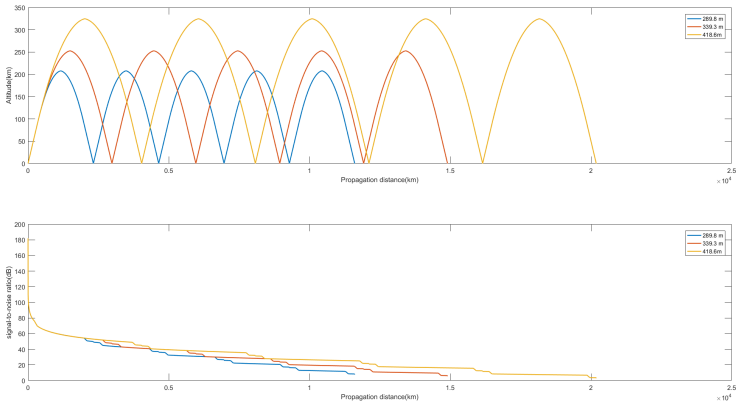

Figure 16: A show of the radio-wave propagation process with the change of the altitude of F layer

7.3 The Wind Speed Near The Sea

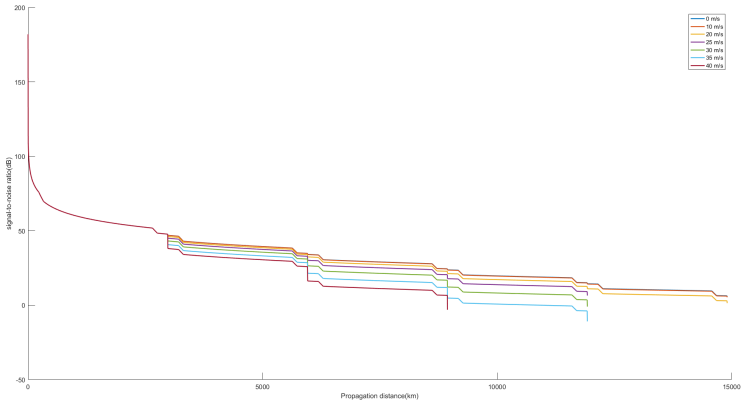

Figure 17: A show of the changes of radio wave energy during propagation with different wind speed

The change of wind speed only affects the sea surface reflectance and does not affect the propagation path of radio waves. **Figure 17** shows the changes in radio wave energy during propagation with different wind speed near the ocean surface. As can be seen from this figure, the increase in wind speed will cause the electromagnetic wave to lose more energy in reflection, and will affect the maximum number of the hops of electromagnetic waves.

8 Strengths and weaknesses

8.1 Strengths

- Our model achieves a good simulation of the process of single-hop and multi-hop propagation for high-frequency radio waves.

- Our model takes into account the effects of calm seas and turbulent seas as well as different terrains.
- The model gives a scheme for the ship to be able to receive the signal continuously, and analyzes the length of the time the ship can remain receiving the signal.
- The model can be widely applied to the design of radio wave propagation path and the decision of frequency.

8.2 Weaknesses

- The parameters that determine the ionospheric properties are taken from Wuhan City and Sanya City and are not representative enough of the rest regions of the Earth.
- The relative permittivity and conductivity of the land surface are approximate with these of the wet concrete, and it may be less accurate to calculate the reflection coefficient of the ground using these data.

References

[1] Marc C. Tarplee. Hf radio wave propagation. http://arrlsc.org/wordpress/Tech%20Presentations/HF%20Radio%20Wave%20Propagation.ppt. [Online; accessed 10-February-2018].

[2] Wikipedia. Skywave. https://en.wikipedia.org/wiki/Skywave. [Online; accessed 11-February-2018].

[3] RF Cafe. Typical daytime ionosphere layer diagram. http://www.rfcafe.com/references/electronics-world/images2/ionospheric-propagation-prediction-electronics-world-april-1969-3.jpg. [Online; accessed 11-February-2018].

[4] Wikipedia. Free-space path loss. https://en.wikipedia.org/wiki/Free-space_path_loss. [Online; accessed 11-February-2018].

[5] A. H Monahan. The probability distribution of sea surface wind speeds. part i: Theory and seawinds observations. *Journal of Climate*, 19(4):502, Feb. 2006.

[6] Wikipedia. Ionosphere. https://en.wikipedia.org/wiki/Ionosphere. [Online; accessed 11-February-2018].

[7] George Simpson. What is a grazing angle? https://www.quora.com/What-is-a-grazing-angle. [Quora; Online; accessed 12-February-2018].

[8] Wikipedia. Boltzmann constant. https://en.wikipedia.org/wiki/Boltzmann_constant. [Online; accessed 12-February-2018].

[9] Wikipedia. Kelvin. https://en.wikipedia.org/wiki/Kelvin. [Online; accessed 12-February-2018].

[10] WANG Ying and GU Jian. Research and simulation analysis of radio reflection characteristic over the ocean. *Electronic Design Engineering*, 24(5):113–119, Mar. 2016.

[11] Reflection from the surface of the earth. https://www.itu.int/pub/R-REP-P.1008.

[12] Yu Chao, Guozhu Shen, Gu Bin, and Guosheng Cheng. Characteristics of electromagnetic wave propagating through ionosphere. *Journal of nanjing information engineering university (natural science edition)*, 5(04):379–384, Aug. 2013.

[13] B. Zolesi and L. R. Cander. Chapter 2: The general structure of the ionosphere, ionospheric prediction and forecasting, springer geophysics. http://www.springer.com/cda/content/document/cda_downloaddocument/9783642384295-c2.pdf?SGWID=0-0-45-1432953-p175163711, Chapter 2:38,2014. [Online; accessed 11-February-2018].

[14] Wikipedia. Snell's law. https://en.wikipedia.org/wiki/Snell%27s_law. [Online; accessed 11-February-2018].

[15] Bertrand Daout, Marc Sallin, and Heinz Wipf. Measurement of complex permittivity of large concrete samples with an open-ended coaxial line. *Measurement Notes*, 10, 2014.

[16] Hamed Layssi, Pouria Ghods, Aali R Alizadeh, and Mustafa Salehi. Electrical resistivity of concrete. *Concrete International*, 37(5):41–46, 2015.

[17] Wikipedia. Electrical resistivity and conductivity. https://en.wikipedia.org/wiki/Electrical_resistivity_and_conductivity. [Online; accessed 12-February-2018].

[18] SUI Gang, HAO Bingyuan, and PENG Lin. Data analysis of topographic relief using standard deviation of elevation (in chinese). *Journal of taiyuan university of technology*, 41(4):383, Jul. 2010.

[19] International Telecommunication Union. Radio noise. https://www.itu.int/dms_pubrec/itu-r/rec/p/R-REC-P.372-13-201609-I!!PDF-C.pdf, 9 2016. P.372-13.

[20] Wikipedia. Decibel watt. https://en.wikipedia.org/wiki/Decibel_watt. [Online; accessed 12-February-2018].

Appendices

Appendix A A Short Synopsis

As an important means of communication, skywave communication is an application of high-frequency radio waves. It uses the reflection of electromagnetic waves between the ionosphere and the surface of Earth to achieve long-distance communication. Multi-hop propagation of high-frequency radio waves is a manifestation of the skywave communication, and can spread farther than single-hop propagation.

In order to simulate the multi-hop propagation process of high-frequency radio waves, a complete mathematical model is established. This model can simulate the reflection between the ionosphere and the surface of Earth, as well as the multi-hop process very well. The ionosphere contains D layer, E layer, F_1 layer and F_2 layer. In the model, we make a reasonable assumption of the daytime ionosphere, combining the actual nature of the ionosphere. We consider the D layer to be a "energy attenuation layer", the E layer as a "single-refraction layer", and the F1 layer and the F2 layer are merged into one layer, F layer, which is considered as a "refraction and reflection layer" .

In order to simulate the attenuation of radio-wave energy during the propagation, we considered three parts, which are the attenuation of energy in the D layer ionosphere, the "free-space path loss" and "energy loss while reflecting off the ground or sea surface" . We also simulate the distribution of electron density and refractive index in the ionosphere along altitude.

Using the Multi-Hop Propagation Model (MHPM), we compare the strength of radio waves after the first reflection off the calm and the turbulent ocean surfaces. And we find that the turbulent sea surface can enhance the attenuation of electromagnetic waves in reflection. We also analyze the maximum number of hops and the maximum propagation distance of several cases with different natural and frequency conditions. In addition, we analyze the change of the ratio of the power in calm-sea case to the power in turbulent-sea case with the grazing angle and the wind speed near ocean surface. Then we find that the power ratio decreases with the increase of the grazing angle and the wind speed .

The MHPM can also be applied to ground-reflection situations very well. We refer to the relevant literature and divide the ground into four categories according to the elevation standard deviation. By studying the change of the ratio of the power in rugged-surface case to smooth-surface case with the standard deviation of elevation, we find that the power decreases rapidly as the elevation standard deviation increasing. What's more, rough ground has a much greater impact on the energy loss of electromagnetic waves than the sea surface. And when the elevation standard deviation is 15, the ground almost loses the ability to reflect electromagnetic waves effectively.

In order to make the ship be able to receive signals continuously while sailing on the sea, we propose a solution and establish the Moving-Ship-Receiving-Signal Model (MSRSM). The solution is to emit electromagnetic waves with a certain bandwidth. We simulate the case with the speed of wind near the sea is $20m/s$, the ship speed is $41.67km/h$, and the frequency range is $21MHz \sim 21.45MHz$, that means that the bandwidth is

$0.45MHz$. The simulation is shown in the following figure. And the length of time the

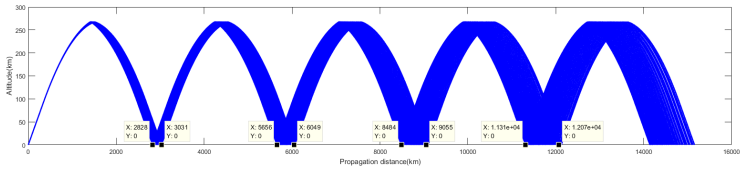

ship can remain receiving signals for each intersection of electromagnetic waves and the sea is shown in the following table.

Intersection zone	Left(km)	Right(km)	Length(km)	Time(hour)
1	2828	3031	203	4.87
2	5656	6049	393	9.43
3	8484	9055	571	13.70
4	11312	12070	758	18.19
total			1925	46.20

The MHPM and MSRSM have good application prospects. They can be used to determine the path, frequency, and grazing angle for the propagation of multi-hop radio waves. Our model can determine the propagation path of radio waves and the change of energy in the course of transmission, for a particular ionosphere with given parameters, the ground or the sea with special physical parameters. Thus, our models are practical. We believe that our model can well simulate the propagation of multi-hop high-frequency radio waves and play a certain role in the field of radio communication.

Appendix B The Code

main.m:

```
clc
clear
%The main program of "multi-hop";
i=1;
D_min=61.2;
D_max=88.6;
E_mid=95.65;
E_max=101;
F_max=271.5;
n1=1;
v=8;  % ocean wind speed, m/s
totalf=[15 17.65 20]; %Define output frequency, MHz
f=totalf(3);
totalAngled=[5 15 25];% grazing angle, degree
for l=1:length(totalf)
    f=totalf(l);
%     angled=totalAngled(l);
    angled=15;
    angle=angled/180*pi;
    x=zeros(1,1);
    y=zeros(1,1);
    Srn=zeros(1,1);
parameterOcean=seareflection(f,angled,v);
lossOcean=parameterOcean(1);
Ploss=lossOcean^2;

NeN_E=calnAndNe(E_mid,f);
n_E=NeN_E(2);

angle_E=acos(cos(angle)*n1/n_E);
p0=100;%transmitting power
       %watt to dBW
dp0=10*log10(p0);%dBW
K_boltzmann=1.38064852e-23; %Boltzmann constant
T0=290;%Kelvin temperature
b=200; %Bandwidth
KT0b=10*log10(K_boltzmann*T0*b);
%Different frequencies correspond to noise levels.
if f==15
    p0=27;
end
if f==17.65
    p0=22;
end
if f==20
    p0=19;
end
pw=10^((p0+KT0b)/10);
dpnoise=10*log10(pw);
Srn(1)=dp0-dpnoise;
SrnLoop(1)=Srn(1);
% Below the ionosphere.
NumLoop=1;
x(1)=0;
y(1)=0;
```

```
dist(1)=0;
k=1;
alpha_D=1.16*10^(-15)*10^10*10^6/f/f;
XofLoop(1)=0;
DISTofLoop(1)=1;
while(SrnLoop(NumLoop)>=10 && NumLoop<=10)
    stepy_D=1;
    while(y(k)<D_min)
        y(k+1)=y(k)+stepy_D;
        x(k+1)=y(k+1)/tan(angle)+XofLoop(NumLoop);
        dist(k+1)=y(k+1)/sin(angle)+DISTofLoop(NumLoop);
        Srn(k+1)=Srn(1)-20*log10(dist(k+1))-20*log10(f)-32.45...
            -alpha_D*(D_max-D_min)/sin(angle)*2*(NumLoop-1)+10*log10(Ploss)...
            *(NumLoop-1);
        k=k+1;
    end
    dist_beforD(NumLoop)=dist(k);
    while(y(k)>D_min && y(k)<=D_max)
        y(k+1)=y(k)+stepy_D;
        x(k+1)=y(k+1)/tan(angle)+XofLoop(NumLoop);
        dist(k+1)=y(k+1)/sin(angle)+DISTofLoop(NumLoop);
        Srn(k+1)=Srn(1)-20*log10(dist(k+1))-20*log10(f)-32.45-alpha_D*(y(k+1)-D_min)...
        /sin(angle)-alpha_D*2*(D_max-D_min)/sin(angle)*(NumLoop-1)+10*log10(Ploss)...
            *(NumLoop-1);
        k=k+1;
    end
    while(y(k)>D_max && y(k)<=E_mid)
        y(k+1)=y(k)+stepy_D;
        x(k+1)=y(k+1)/tan(angle)+XofLoop(NumLoop);
        dist(k+1)=y(k+1)/sin(angle)+DISTofLoop(NumLoop);
        Srn(k+1)=Srn(1)-20*log10(dist(k+1))-20*log10(f)-32.45-alpha_D*(D_max-D_min)...
        /sin(angle)-alpha_D*(D_max-D_min)/sin(angle)*2*(NumLoop-1)+10*log10(Ploss)...
            *(NumLoop-1);
        k=k+1;
    end
    x_beforeE_mid(NumLoop)=x(k);
    y_beforeE_mid(NumLoop)=y(k);
    dist_beforeE(NumLoop)=dist(k);
    while(y(k)>=E_mid && y(k)<=E_max)
        y(k+1)=y(k)+stepy_D;
        x(k+1)=x_beforeE_mid(NumLoop)+(y(k+1)-y_beforeE_mid(NumLoop))/tan(angle_E);
        dist(k+1)= dist_beforeE(NumLoop)+(y(k+1)-y_beforeE_mid(NumLoop))/sin(angle_E);
        Srn(k+1)=Srn(1)-20*log10(dist(k+1))-20*log10(f)-32.45-alpha_D*(D_max-D_min)...
        /sin(angle)-alpha_D*(D_max-D_min)/sin(angle)*2*(NumLoop-1)+10*log10(Ploss)...
            *(NumLoop-1);

        k=k+1;
    end
    stepy_F=0.01;
    t=1;
    NeN_F=calnAndNe(y(k),f);
    n_F(1)=NeN_F(2);
    cosAngleF=cos(angle_E);
    COSF(1)=cosAngleF;
    while(y(k)>=E_max && y(k)<=F_max && cosAngleF<1 && (1-cosAngleF)>0.0001)
        y(k+1)=y(k)+stepy_F;
        NeN_F=calnAndNe(y(k+1),f);
        n_F(t+1)=NeN_F(2);
        cosAngleF=COSF(t)*n_F(t)/n_F(t+1);
```

```
        COSF(t+1)=cosAngleF;
        angle_F=acos(cosAngleF);
        AF(t)=angle_F;
        x(k+1)=x(k)+stepy_F/tan(angle_F);
        dist(k+1)=dist(k)+stepy_F/sin(angle_F);
        Srn(k+1)=Srn(1)-20*log10(dist(k+1))-20*log10(f)-32.45-alpha_D*(D_max-D_min)...
        /sin(angle)-alpha_D*(D_max-D_min)/sin(angle)*2*(NumLoop-1)+10*log10(Ploss)...
            *(NumLoop-1);
        k=k+1;
        t=t+1;
    end
    [dimx,rdimy]=size(x);
    dimy=(rdimy)/(2*NumLoop-1);
    for j=1:dimy
        x(rdimy+j)=-x(rdimy-j+1)+2*x(rdimy);
        y(rdimy+j)=y(rdimy-j+1);
    end
    for j=rdimy+1:rdimy+dimy

        dist(k+1)=dist(k)+sqrt((x(j)-x(j-1))^2+(y(j)-y(j-1))^2);
        Srn(k+1)=Srn(1)-20*log10(dist(k+1))-20*log10(f)-32.45-alpha_D*(D_max-D_min)...
        /sin(angle)-alpha_D*(D_max-D_min)/sin(angle)*2*(NumLoop-1)+10*log10(Ploss)...
            *(NumLoop-1);
        if(y(k)>D_max && y(k+1)<=D_max)
            distD=dist(k+1);
        end
        if (y(k+1)<=D_max && y(k+1)>=D_min)
            Srn(k+1)=Srn(k+1)-alpha_D*(dist(k+1)-distD);
        end
        if(y(k+1)<=D_min)
            Srn(k+1)=Srn(k+1)-alpha_D*(D_max-D_min)/sin(angle);
        end
        k=k+1;
    end
    DISTofLoop(NumLoop+1)=dist(k);
    XofLoop(NumLoop+1)=x(k);
    SrnLoop(NumLoop+1)=Srn(k);
    x(k+1)=x(k);
    y(k+1)=y(k);
    y(k+1)=0;
    dist(k+1)=dist(k);
    Srn(k)=Srn(k)+10*log10(Ploss);
    Srn(k+1)=Srn(k);
    k=k+1;
    NumLoop=NumLoop+1;
end
subplot(2,1,1)
% colormap('Hot')
% patch([x NaN],[y NaN],[Srn Srn(end)],'edgecolor','flat','facecolor','none')
plot(x,y,'linewidth',1.5);
xlabel('Propagation distance(km)')
ylabel('Altitude(km)')

hold on
% colorbar
subplot(2,1,2)
% patch([x NaN],[Srn NaN],[Srn Srn(end)],'edgecolor','flat','facecolor','none')
plot(x,Srn,'linewidth',1.5);
xlabel('Propagation distance(km)')
```

```
ylabel('signal-to-noise ratio(dB)')

hold on
end
colormap('hsv')
subplot(2,1,1)
 legend('15 MHz','17.65 MHz','20 MHz');
% legend('5^o','15^o','25^o');
subplot(2,1,2)
 legend('15 MHz','17.65 MHz','20 MHz');
% legend('5^o','15^o','25^o');
```

calnAndNe.m:

```
function NeN=calnAndNe(h,f)
%this function is a simulatation of the n and NeãĂĆ
%And the 'h' should above the ionosphere 'E'.
f_0E=3.21;  %MHz
h_mE=101;   %km
y_mE=10.7;  %km
f_0F2=14.20;%MHz
h_mF2=339.3;%km
y_mF2=78; %km
f_j=1.7*f_0E;
N_j=1.24/100*f_j^2;%10^12* m^(-3)
h_j=h_mF2-y_mF2*sqrt(1-(f_j/f_0F2)^2);
N_mE=3.16/100;%10^12* m^(-3)
N_mF2=2.5;%10^12* m^(-3)
H=1.66*(30+0.075*(h_mF2-200));
NeN=zeros(1,2);
if h < (h_mE-y_mE) || h > 1000
    n=100; %means the "h" is not in the effective range
    Ne=0; %means the "h" is not in the effective range
end
if h >= (h_mE-y_mE) && h <= h_mE
    Ne=N_mE*(1-((h-h_mE)/y_mE)^2);
    n=sqrt(1-80.8*Ne/f/f);
end
if h > h_mE && h <= h_j
    Ne=(N_j-N_mE)/(h_j-h_mE)*h+(N_mE*h_j-N_j*h_mE)/(h_j-h_mE);
    n=sqrt(1-80.8*Ne/f/f);
end
if h > h_j && h <= h_mF2
    Ne=N_mF2*(1-((h-h_mF2)/y_mF2).^2);
     n=sqrt(1-80.8*Ne/f/f);
end
if h > h_mF2 && h <= 1000
    Ne=N_mF2*exp(0.5*(1-(h-h_mF2)/H-exp(-1.0*(h-h_mF2)/H)));
    n=sqrt(1-80.8*Ne/f/f);
end
NeN(1)=Ne;
NeN(2)=n;
```

fcandMUF.m:

```
function frequency=fcandMUF(Ne,h)
R=6371;%The radius of the earth,km
fcr=(Ne/1.24/10^10).^(0.5);%Critical frequency;
MUF=fcr/(1-(R/(R+h)).^2).^0.5;
```

```
frequency=[fcr,MUF];
end
```

groundreflection.m:

```
function f=groundreflection(fre,angle,Sh)
theta=15;
thgema=0.05;
lamda=3*10^2/fre;
retheta=theta+lamda*thgema*60i;
Rh=(sind(angle)-(retheta-(cosd(angle)).^2).^0.5)/(sind(angle)+...
    (retheta-(cosd(angle)).^2).^0.5);
Rv=(retheta*sind(angle)-(retheta-(cosd(angle)).^2).^0.5)/...
    (retheta*sind(angle)+(retheta-(cosd(angle)).^2).^0.5);
Rh=abs(Rh);
Rv=abs(Rv);
g=4*pi*Sh/lamda*sind(angle);
thou=exp(-1/(2*g.^2));
Rhrough=Rh*thou;
Rvrough=Rv*thou;
f=[Rh,Rv,Rhrough,Rvrough];
end
```

seareflection.m:

```
function f=seareflection(fre,angle,v)
% a=1.411*10^-2;
% b=-5.212*10^-8;
% c=5.854*10^-11;
% d=-7.671*10^-16;
% e=2.985*10^-21;
% theta(i,1)=1/(a+b*fre+c*fre.^2+d*fre.^3+e*fre.^4);
% r=3.858;
% s=9.125*10^-4;
% t=1.530*10^-8;
% u=-2.117*10^-5;
% v=6.572*10^-10;
% w=-1.964*10^-15;
% thgema(i,1)=(r+s*fre+t*fre.^2)/(1+u*fre+v*fre.^2+w*fre.^3);
theta=70;
thgema=5;
lamda=3*10^2/fre;
retheta=theta+lamda*thgema*60i;
Rh=(sind(angle)-(retheta-(cosd(angle)).^2).^0.5)/(sind(angle)+...
    (retheta-(cosd(angle)).^2).^0.5);
Rv=(retheta*sind(angle)-(retheta-(cosd(angle)).^2).^0.5)/...
    (retheta*sind(angle)+(retheta-(cosd(angle)).^2).^0.5);
Rh=abs(Rh);
Rv=abs(Rv);
h=0.0051*v.^2;
g=0.5*(4*pi*h*fre*10^6*sind(angle)/3/10^8)^2;
thou=1/(3.2*g-2+((3.2*g)^2-7*g+9).^0.5)^0.5;
Rhrough=Rh*thou;
Rvrough=Rv*thou;
f=[Rh,Rv,Rhrough,Rvrough];
end
```

tryfcandMUF.m:

```
clc
clear
% try fcandMUF.m
h_f=339-30:339;
f=10;
[dimx,dimy]=size(h_f);
for i=1:dimy
    NeN(i,:)=calnAndNe(h_f(i),f);
    fre(i,:)=fcandMUF(NeN(i,1)*10^12,h_f(i));
end
% plot(fre(:,1),h_f);
% xlabel('fc')
% ylabel('h(km)')
% figure(2)
plot(fre(:,2),h_f);
xlabel('MUF(MHz)')
ylabel('h(km)')
```

tryforCalnAndNe.m:

```
clc
clear
% try calnAndNe.m
f=15;
h=91:1:600;
[dimx,dimy]=size(h);
NeN=zeros(dimy,2);
for i=1:dimy
    NeN(i,:)=calnAndNe(h(i),f);
end
figure(1)
plot(NeN(:,1),h);
xlabel('10^1^2 m^-^3')
ylabel('h(km)')
figure(2)
plot(NeN(:,2),h);
```